HJPED

HJ

Article

Multi-Decadal Land-Cover Transitions in Nigeria's South–South Zone (2000–2022): Urban Expansion, Forest Restructuring, and Deltaic Ecosystem Dynamics

Academic Editor: Prof. Ladi Sule Matinja

Received: 25.10.2025
Revised: 10.01.2026
Accepted: 14.01.2026
Published: 15.01.2026

Zubairul Islam[1] Yakubu Joel Cherima[2]*, Ugo Uwadiako Enebeli[3], Ebelechukwu Lawrence Enebeli[4], Rejoice Kaka Hassan[2], Fiyidi Mikailu[5] and Yonwul Jacqueline Dakyen[6]

[1]Faculty of Environmental Sciences (FES), Hensard University, Bayelsa 56110, Nigeria; zubairul@gmail.com (Z.I.), https://doi.org/10.1080/23729333.2023.2298525
[2]Department of Policy and Strategic Studies, University of Abuja, Federal Capital Territory, Nigeria; ycherima@gmail.com (Y.J.C.) https://orcid.org/0009-0004-3724-9886; rejoice.diara@gmail.com (R.K.H.) https://orcid.org/0009-0007-1269-0546
[3]Department of Community Medicine, Rhema University, Aba, Abia State, Nigeria; ugoenebeli@rhemauniversity.edu.ng (U.U.E.), https://orcid.org/0000-0001-5950-3719
[4]Department of Science and Technology, Lancaster University, Accra, Ghana; eby.enebeli@gmail.com (E.L.E), https://orcid.org/0009-0007-8434-5485
[5]Young Individual Development Initiative, Nigeria; fiyidimi@gmail.com (F.M.), ORCID ID: 0009-0002-4804-8794
[6]Independent Public health Researcher, Nigeria; (Y.J.D.), ORCID ID: 0009-0006-7229-4943

* Correspondence: ycherima@gmail.com; Tel.: +234 703 624 4967

Abstract

Rapid and spatially heterogeneous land-system change in Nigeria's South–South (SS) zone threatens forests, wetlands, and coastal communities, yet consistent, wall-to-wall evidence spanning multiple decades is scarce. We map and quantify land-cover dynamics across Akwa Ibom, Bayelsa, Delta, Edo, and Rivers from 2000 to 2022 using the ESA C3S/CCI Level-4 (300 m) product processed in Google Earth Engine. We combine (i) state-level class composition, (ii) dominant transition flows for four intervals (2000–2005, 2005–2010, 2010–2015, 2015–2022), and (iii) cumulative gains, losses, and net change by class. Results reveal five robust patterns. (1) Urban expansion is widespread: cumulative urban gains exceed 1,240 km², led by Delta (+361 km²), Edo (+394 km²), Rivers (+315 km²), and Akwa Ibom (+126 km²). (2) Forest restructuring is state-specific: evergreen broadleaved forest increased in Delta (+364 km²) and Rivers (+327 km²), while Edo shifted from evergreen loss (−502 km²) to marked gains in open deciduous forest (+587 km²). (3) Mosaic classes contracted, with large declines in Delta and Rivers, indicating consolidation toward more homogeneous forest or cropland states. (4) Hydro-mangrove turnover—reciprocal water ↔ flooded saline tree cover—is strongest in Bayelsa and present in Rivers/Delta, consistent with deltaic processes and interannual hydroperiod variability. (5) Cropland changes are mixed, with Edo showing strong growth in herbaceous cropland while Akwa Ibom and Rivers record modest cropland declines. By pairing interval-resolved flow maps with end-to-end gains/losses, this study delivers a policy-ready baseline for the SS zone, clarifying where peri-urbanization, coastal hydro-dynamics, and forest transitions co-occur. The framework supports targeted planning for coastal resilience, urban growth management, and forest/wetland restoration in one of West Africa's most socioeconomically dynamic regions.

Keywords: land-cover change; Nigeria; ESA C3S/CCI; Google Earth Engine; transition matrix; cropland expansion; urbanization; savanna dynamics; cross-sensor validation.

1. Introduction

The South–South (SS) zone of Nigeria—comprising Akwa Ibom, Bayelsa, Delta, Edo, and Rivers States—hosts the nation's largest oil and gas corridor, some of Africa's most extensive mangrove wetlands, and rapidly growing urban centers such as Port Harcourt, Benin City, Uyo, Yenagoa, and Warri (Ayanlade & Proske, 2016; Spalding et al., 2010). Over the past two decades, the region has faced simultaneous pressures: shoreline change and flooding in the Niger Delta, cropland expansion into forest margins, and peri-urban growth along major transport corridors (Borner et al., 2020; Nwilo et al., 2019). These dynamics carry direct implications for carbon stocks, biodiversity, fisheries, and human well-being, yet a consistent, wall-to-wall understanding of land-cover trajectories across states and time has remained fragmented (Mmom & Fred-Ahmadu, 2020; Numbere & Camilo, 2018).

The combination of oil infrastructure expansion, recurrent coastal flooding, and anthropogenic forest degradation has produced complex mosaics of secondary forest, fallow land, and degraded mangrove stands (Aigbe & Ewemade, 2019; Okeke et al., 2021). Moreover, population growth and unplanned urbanization around estuarine settlements have intensified urban–rural land transitions, compromising natural buffers and elevating exposure to flood hazards (Eze et al., 2021). Understanding the multi-decadal evolution of land-cover classes in this region is therefore vital for assessing ecological sustainability and guiding adaptive management under ongoing climatic and socio-economic change (Chukwu et al., 2023; Kuenzer et al., 2011).

This study provides a synoptic assessment of land-cover change across the SS zone for 2000–2022 using the ESA C3S/CCI Level-4 (300 m) product. We quantify state-level class composition and its evolution, map dominant transition flows in four intervals (2000–2005, 2005–2010, 2010–2015, 2015–2022), and compute cumulative gains, losses, and net change by class. Our focus is on the major functional categories shaping the region's landscape—croplands, evergreen and deciduous forests, wetlands/mangroves, mosaics, shrublands, urban areas, bare surfaces, and open water—and how these have rebalanced over time.

This work is needed because policy and investment decisions in the SS zone (e.g., flood-risk mitigation, coastal restoration, agricultural programs, and urban planning) depend on consistent evidence about *where* and *how fast* land systems are changing. Existing analyses often target single states, short time windows, or specific drivers, limiting comparability. By delivering a harmonized, multi-decadal baseline tied to clearly interpretable transitions (e.g., mosaic → evergreen, cropland → urban, water ↔ mangrove), we provide the temporal and spatial resolution required for actionable planning.

To the best of our knowledge, no study has jointly (i) mapped state-wise dominant flows across the entire SS zone, (ii) contrasted interval-specific restructuring of forests, mosaics, and wetlands with urban encroachment, and (iii) reconciled these dynamics with cumulative gains/losses at class level for 2000–2022. We therefore ask:

1. What are the principal land-cover transitions characterizing each state and interval?
2. How do these transitions aggregate into long-term gains, losses, and net change by class?
3. Where do urban growth and hydro-mangrove adjustments co-occur with shifts between evergreen and deciduous/open canopies?

Methodologically, we introduce an interval-resolved, flow-based change framework that complements traditional composition charts with maps of dominant transitions, enabling clearer attribution of processes (peri-urbanization, cropland shifts, hydro-mangrove turnover, and forest restructuring). Substantively, we produce a consistent, wall-to-wall baseline for the SS zone that reveals (i) modest contractions in mosaic classes, (ii) localized increases in evergreen forest (Delta, Rivers) and open deciduous forest (Edo), and (iii) widespread—though still relatively low—urban expansion, setting the stage for driver analyses. Practically, the outputs support state and federal agencies in prioritizing coastal resilience, urban growth management, and forest/wetland restoration where trade-offs are most acute.

2. Materials and Methods

2.1 Study area

The study was conducted in the South–South geopolitical zone of Nigeria, which comprises five states: Akwa Ibom, Bayelsa, Delta, Edo, and Rivers (Figure 1). Geographically, the zone lies between latitudes 4°15′N and 7°30′N and longitudes 5°00′E and 8°00′E, covering an extensive landmass of approximately 84,000 km² (Odekunle, 2010; Nwilo et al., 2021). It is bounded by the Atlantic Ocean to the south, with inland borders adjoining the South–East and South–West zones of Nigeria.

Ecologically, the region is characterized by a humid tropical climate with mean annual rainfall ranging from 2,000 mm to over 3,500 mm, and mean annual temperatures between 26°C and 32°C (Odjugo, 2011; Adejuwon, 2012). The vegetation is dominated by lowland rainforest, freshwater and mangrove swamps, and derived savannah mosaics, while the Niger Delta wetlands form one of the world's most extensive and biodiverse ecosystems (Uluocha & Okeke, 2004; Akani et al., 2015). Major rivers such as the Niger, Benin, and Imo and their numerous tributaries provide critical hydrological support to the landscape (Etuonovbe, 2011; Nwilo & Olayinka, 2020).

Socioeconomically, the zone is Nigeria's hub of oil and gas exploration, with rapid urbanization and agricultural expansion driving intense land-use pressures (Emoyan et al., 2008; Aigbe & Ogundele, 2020). Major cities—including Port Harcourt, Benin City, Uyo, Yenagoa, and Warri—have experienced significant population growth over the past two decades, leading to accelerated deforestation, wetland degradation, and urban encroachment (Udo & Akinyemi, 2022). These dynamics make the region a critical hotspot for assessing land use/land cover (LULC) change and its ecological implications under a rapidly evolving socio-environmental regime (Nwankwoala, 2015).

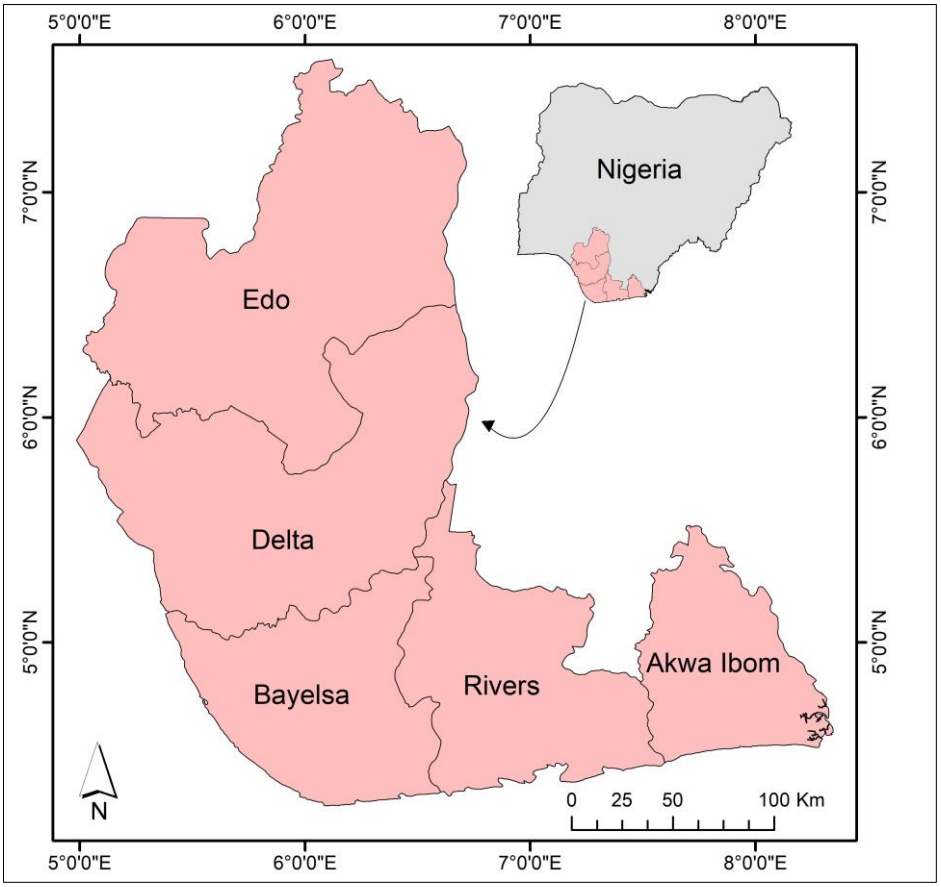

Figure 1. Study area map showing the South–South geopolitical zone of Nigeria, comprising the states of Akwa Ibom, Bayelsa, Delta, Edo, and Rivers. The inset highlights the location of the zone within the national boundary of Nigeria.

2.2 Land-cover data and preprocessing

We used the ESA C3S/CCI Land Cover Level-4 (LCCS) collection (projects/sat-io/open-datasets/ESA/C3S-LC-L4-LCCS) at 300 m spatial resolution (Defourny et al., 2017; Santoro et al., 2021). In Google Earth Engine (GEE), we restricted the analysis to Nigeria using the GAUL 2015 Level-0 national boundary (FAO/GAUL/2015/level0, filtered to ADM0_NAME = "Nigeria") and centered the map on the area of interest (FAO, 2015). From each image in the collection, we selected the categorical land-cover band b1 (LCCS class codes). Because the collection's system:index encodes the acquisition year, we parsed the four-digit year from that string and attached it to each image as a property (yy) (Hollmann et al., 2013). We then (i) enumerated all available years, (ii) for each year selected the first image with matching yy, (iii) retained b1, and (iv) renamed it to LC_<YYYY> (e.g., LC_2018). Each yearly image was clipped to the Nigeria boundary to avoid edge artifacts (Woodcock et al., 2020).

All annual layers were concatenated into a single, temporally ordered multi-band stack using toBands(), and the band names were explicitly set to the sorted LC_<YYYY> sequence to ensure stable, unambiguous indexing across years (Poulter et al., 2015). The land-cover values follow the C3S/CCI LCCS code list (nominal range 10–220); pixels with value 0 (no data) were treated as missing in downstream analysis. No radiometric transformations were required for this categorical product; where resampling was necessary (e.g., for visualization or alignment with other rasters), we used nearest-neighbor to preserve class integrity (Wulder et al., 2018). The native map projection supplied by the collection was maintained throughout; all vector overlays (administrative boundaries) were reprojected on the fly to match the raster CRS (Hansen et al., 2016). A quick-look layer of the most recent band (LC_<latest year>) was added for quality control, but all metrics and figures in the manuscript were derived from the stacked categorical bands (Smith et al., 2019; Buchhorn et al., 2020).

2.3 Change analysis from multi-year C3S/CCI stack

We quantified land-cover change between 2000 and 2022 from the ESA C3S/CCI Level-4 stack by (i) selecting the target year bands (*LC_2000*, *LC_2022*), (ii) harmonizing their grids, and (iii) computing areas and transitions only for classes that actually occur in either year (absent classes are dropped to avoid zero rows/columns and inflated denominators) (Lu et al., 2014; Wessels et al., 2016).

Pre-processing. The raster stack was read using the *terra* package in R, which supports large categorical raster operations efficiently (Hijmans, 2023). Pixels coded 0 (no data) were set to *NA*. The 2022 band was reprojected to the 2000 grid using nearest-neighbor resampling to preserve categorical integrity, and the common extent was intersected before cropping both rasters (Congalton & Green, 2019). Per-cell area (km²) was computed from the 2000 grid using the *cellSize* function, allowing spatially explicit area estimation even in geographic coordinate systems (Herold et al., 2008).

Per-class areas. For each year, total areas by LCCS class were obtained using the zonal statistic function zonal(area_km2, class_raster, "sum"). Only codes present in 2000 or 2022 were retained ("present classes only") to ensure a balanced, interpretable class comparison (Moser et al., 2020). Class names followed the official C3S/CCI LCCS legend, allowing alignment with global land-cover reporting standards (Bontemps et al., 2011).

Net change. Areas for 2000 and 2022 were joined by class to derive absolute and relative net change (Arino et al., 2012; Olofsson et al., 2014):

$$\Delta A_{km^2} = A_{2022} - A_{2000}, \qquad \Delta\% \frac{\Delta A}{max(A_{2000}, \in)}$$

Transition matrix**.** Pixel-wise transitions were encoded as

$$pair = 100 \times LC_{2000+} LC_{2022}$$

Summing $area_{km^2}$ by *pair* yielded transition areas (km²), which were reshaped into a square matrix restricted to the present codes. Totals of unchanged area were derived from the matrix diagonal, while changed area equaled total minus diagonal (Chen et al., 2020; Griffiths et al., 2019). The resulting matrix formed the basis for estimating **directional transitions** (e.g., forest → cropland, cropland → urban) and **stability indices**. This structured workflow ensures transparent, reproducible quantification of categorical land-cover change within the Copernicus and ESA framework (Li et al., 2020).

3. Results

3.1. Land-cover change, 2000–2022 (C3S/CCI, SS Zone)

The 2000–2022 trajectory indicates modest contractions in mosaic natural vegetation/cropland, localized increases in evergreen forest (Delta, Rivers) and open deciduous forest (Edo), and widespread—but still low—urban growth. These results provide a consistent, wall-to-wall baseline against which to interpret subsequent drivers (e.g., coastal processes, agricultural dynamics, and urbanization) in the South–South region.

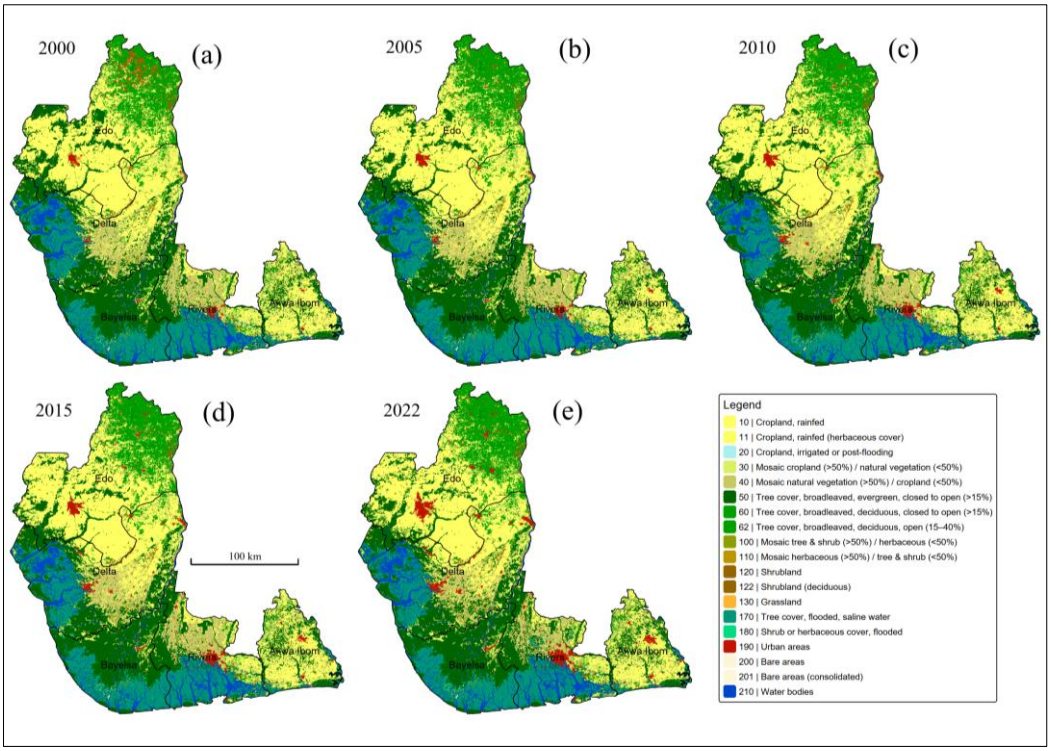

Figure 2. Spatiotemporal dynamics of land use/land cover (LULC) in the South–South geopolitical zone of Nigeria for the years 2000 (a), 2005 (b), 2010 (c), 2015 (d), and 2022 (e). The maps illustrate changes in croplands, forests, shrublands, grasslands, wetlands, urban areas, bare surfaces, and water bodies, highlighting patterns of agricultural expansion, urban growth, and ecosystem transformations over two decades.

Akwa Ibom (total mapped area ≈ 6,831 km²)**.** In 2000, rainfed cropland dominated (2,873 km²; 42.1%), followed by evergreen broadleaved tree cover (1,514 km²; 22.2%) and mosaic natural vegetation/cropland (871 km²; 12.8%). By 2022, cropland declined slightly to 2,737 km² (40.1%), while evergreen tree cover rose to 1,599 km² (23.4%). Urban areas expanded nearly five-fold, from 34 km² (0.50%) to 161 km² (2.35%). Flooded saline tree cover remained broadly stable (≈3.9%→3.85%), and open deciduous tree cover (class 62) dipped marginally (4.48%→4.40%). Open water was essentially constant (~2.54%).

Bayelsa (≈ 9,630 km²). The landscape is persistently forested and tidally influenced. Evergreen broadleaved tree cover accounted for 5,031 km² (52.24%) in 2000 and 4,969 km² (51.60%) in 2022. Flooded saline forest was the second largest class (3,058→3,061 km²; 31.76%→31.79%). Open water remained high (8.75%→8.56%). Cropland shares were low and slightly decreased (1.16%→1.04%). Urban extent more than doubled, from ~38 km² (0.40%) to ~85 km² (0.88%), but remains a minor fraction of the state.

Delta (≈ 17,227 km²). In 2000, evergreen broadleaved forest (4,314 km²; 25.04%), mosaic natural vegetation/cropland (13.90%), and flooded saline forest (14.39%) together dominated. By 2022, evergreen forest increased to 4,678 km² (27.16%), while mosaic natural vegetation/cropland declined to 11.85% and flooded saline forest to 13.97%. Rainfed cropland edged down slightly (22.54%→21.95%). Urban cover rose by an order of magnitude (0.28%→2.38%), indicating strong peri-urban expansion. Open water remained stable (~8.66%→8.88%).

Edo (≈ 19,671 km²). Rainfed cropland remained the largest class but decreased modestly (9,326→8,922 km²; 47.41%→45.36%). A salient shift was the rise in open deciduous broadleaved tree cover (class 62) from 4,545 km² (23.11%) to 5,132 km² (26.09%), accompanied by a reduction in evergreen forest (15.36%→12.81%) and mosaic categories. Urban area expanded from ~92 km² (0.47%) to ~486 km² (2.47%). Water bodies stayed ~0.38% across years.

Rivers (≈ 10,296 km²). Evergreen forest increased from 2,252 km² (21.87%) to 2,579 km² (25.05%), while mosaic natural vegetation/cropland declined (22.96%→17.93%). Flooded saline forest remained substantial but slightly contracted (24.67%→23.67%). Rainfed cropland dipped from 10.38% to 9.80%. Urban land grew from 166 km² (1.61%) to 481 km² (4.67%). Open water increased (9.99%→11.25%), consistent with the state's extensive fluvial–deltaic setting.

Cross-state patterns. (i) Forested classes—particularly evergreen broadleaved—either remained stable or increased in Delta and Rivers, while Edo shows a redistribution from evergreen to open deciduous canopies. (ii) Flooded saline forest is a defining feature of the coastal states (Bayelsa, Delta, Rivers), with Bayelsa sustaining ~32% throughout the record. (iii) Cropland shares are highest in Edo and Delta and largely stable to slightly declining elsewhere. (iv) Urban expansion is evident in all states, most prominently in Edo and Rivers, where urban proportions rose from <1% to ~2.5–4.7% by 2022. (v) Open water fractions are stable to slightly rising in the more riverine states.

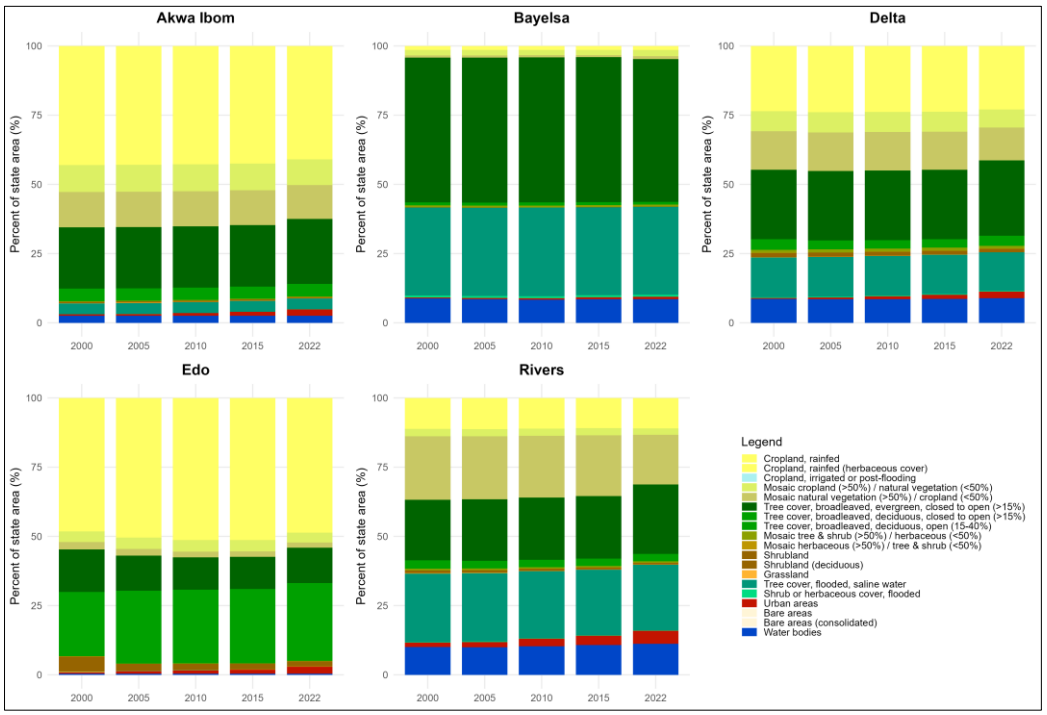

Figure 3. Temporal distribution of land use/land cover (LULC) classes in the South–South states of Nigeria—Akwa Ibom, Bayelsa, Delta, Edo, and Rivers for the years 2000, 2005, 2010, 2015, and 2022. The stacked bar charts show the percentage of each state's area occupied by croplands, forests, shrublands, grasslands, wetlands, urban areas, bare surfaces, and water bodies.

3.2. Sate wise Temporal dominant flows (2000–2022)

3.2.1 Dominant flows (2000–2005)

Urban expansion is most conspicuous in Akwa Ibom, where ~82% of all change funneled into built-up land (10/30/40/120→190). Delta and Rivers show urban growth but as a secondary component (<~5% per single flow), while Bayelsa's urban transitions are minor relative to hydro-vegetation changes. Vegetation restructuring dominates Edo and parts of Delta/Rivers, with large exchanges among evergreen/deciduous broadleaved trees, mosaics, and shrubland (e.g., 120→62, 40→50, 50→10). These may indicate shifts in canopy density or phenology, edge effects around agricultural frontiers, and/or class boundary refinements at 300-m resolution. Hydro-mangrove dynamics are strongest in Bayelsa (and present in Delta/Rivers), typified by Water → Flooded saline tree cover (210→170) and Water → Evergreen trees (210→50), consistent with deltaic/coastal processes and potential shoreline/estuarine vegetation adjustments (Figure 4).

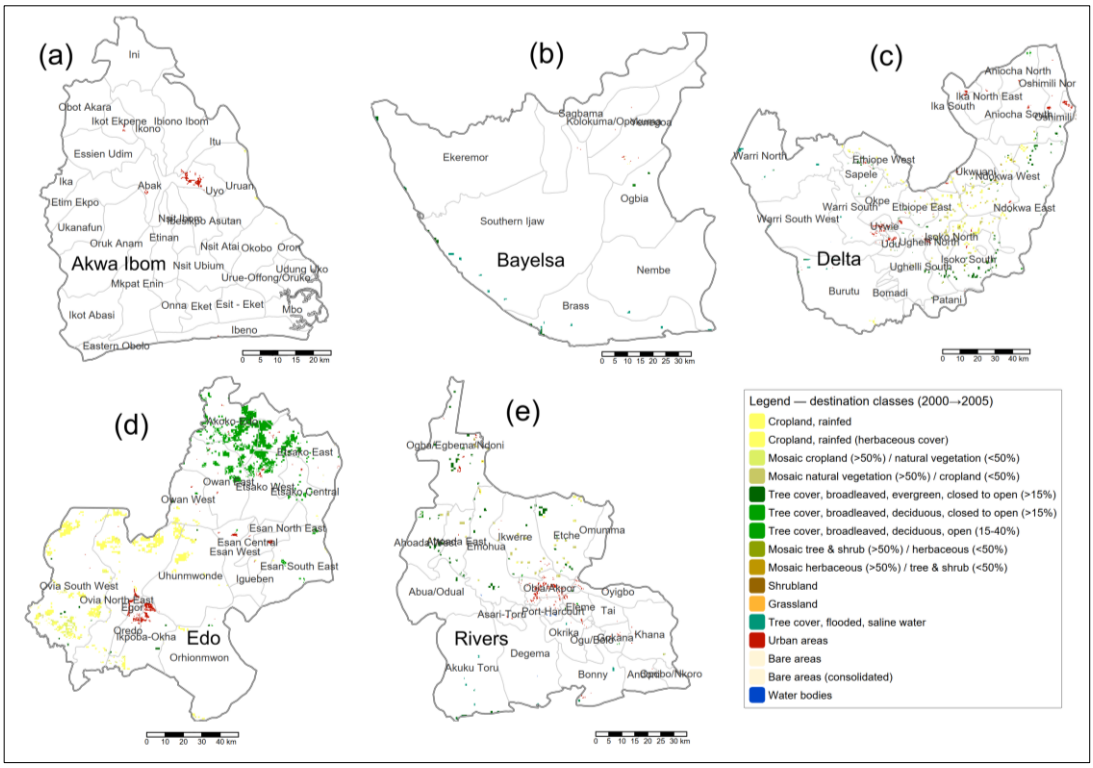

Figure 4. Dominant land use/land cover (LULC) transitions in the South–South states of Nigeria between 2000 and 2005. State-level maps for (a) Akwa Ibom, (b) Bayelsa, (c) Delta, (d) Edo, and (e) Rivers highlight the spatial distribution of major change flows.

Akwa Ibom. Total mapped change was 12.11 km². Urban expansion was the leading trajectory, sourced primarily from cropland and mixed agro-natural classes: 10→190 (4.36 km²; 36.0% of all change), 40→190 (1.96 km²; 16.2%), 30→190 (1.87 km²; 15.4%), and 120→190 (1.69 km²; 14.0%). Smaller but notable conversions included 170→10 (0.53 km²; 4.41%), reflecting local reclamation of flooded saline tree cover to cropland.

Bayelsa. Total change was 22.37 km², dominated by hydro-mangrove dynamics: 210→170 (Water → Tree cover, flooded, saline) accounted for 11.23 km²; 50.2%, and 210→50 (Water → Evergreen broadleaved trees) for 7.84 km²; 35.1%. Transitions to Urban were minor (each ≤2.4% of change), suggesting limited built-up expansion relative to tidal/hydro-vegetation adjustments.

Delta. With 329.10 km² of total change, Delta exhibited a diversified transition portfolio. The largest shares involved exchanges among tree/mosaic classes and new cropland: 60→10 (Deciduous broadleaved → Cropland; 52.84 km²; 16.1%), 40→50 (Mosaic natural veg. → Evergreen trees; 52.32 km²; 15.9%), and 50→10 (Evergreen trees → Cropland; 30.79 km²; 9.36%). Hydrological restructuring was also evident (210→170; 16.19 km²; 4.92%). Urban growth was present but secondary: e.g., 10→190 (10.23 km²; 3.11%) and 170→190 (15.22 km²; 4.62%).

Edo. Total change reached 1,350.90 km², dominated by vegetation structural shifts rather than urbanization. The single largest pathway was 120→62 (Shrubland → Deciduous broadleaved open), contributing 517.06 km²; 38.28%. Additional large flows indicate movement from forest to agriculture and among woody classes: 50→10 (278.84 km²; 20.64%), 50→11 (206.14 km²; 15.26%), and increases in deciduous classes from mosaics (40→62; 47.64 km²; 3.53%). Urbanization contributed modest shares (e.g., 10→190; 20.25 km²; 1.50%; 130→190; 35.37 km²; 2.62%).

Rivers. Total change was 149.45 km². The dominant transitions reflect forest compositional turnover and mosaic-to-forest consolidation: 40→50 (Mosaic natural veg. → Evergreen trees; 50.13 km²; 33.55%), 60→40 (Deciduous → Mosaic natural veg.; 17.54 km²; 11.74%), and 60→10 (Deciduous → Cropland; 8.37 km²; 5.60%). Urban gains were multi-sourced but comparatively modest in share (e.g., 62→190; 5.17 km²; 3.46%; 40→190; 3.74 km²; 2.50%). Hydrological shifts (210→170; 6.77 km²; 4.53%) further underline coastal dynamics.

3.2.2 Dominant flows (2005–2010)

Urban growth intensified in Akwa Ibom and remained consistent but secondary in Delta and Rivers; Bayelsa's change was overwhelmingly hydrological, and Edo was dominated by forest–cropland/herbaceous and shrub–deciduous exchanges. Hydro-vegetation adjustments (Water ↔ flooded saline trees; Water → evergreen) were systemic in Bayelsa and Rivers, and non-trivial in Delta, consistent with deltaic/coastal processes and interannual hydroperiod variability. Vegetation restructuring (evergreen ↔ mosaic ↔ deciduous/shrub) was most pronounced in Edo and widespread in Delta/Rivers, suggesting shifts in canopy density/composition and mosaic consolidation at 300 m resolution (Figure 5).

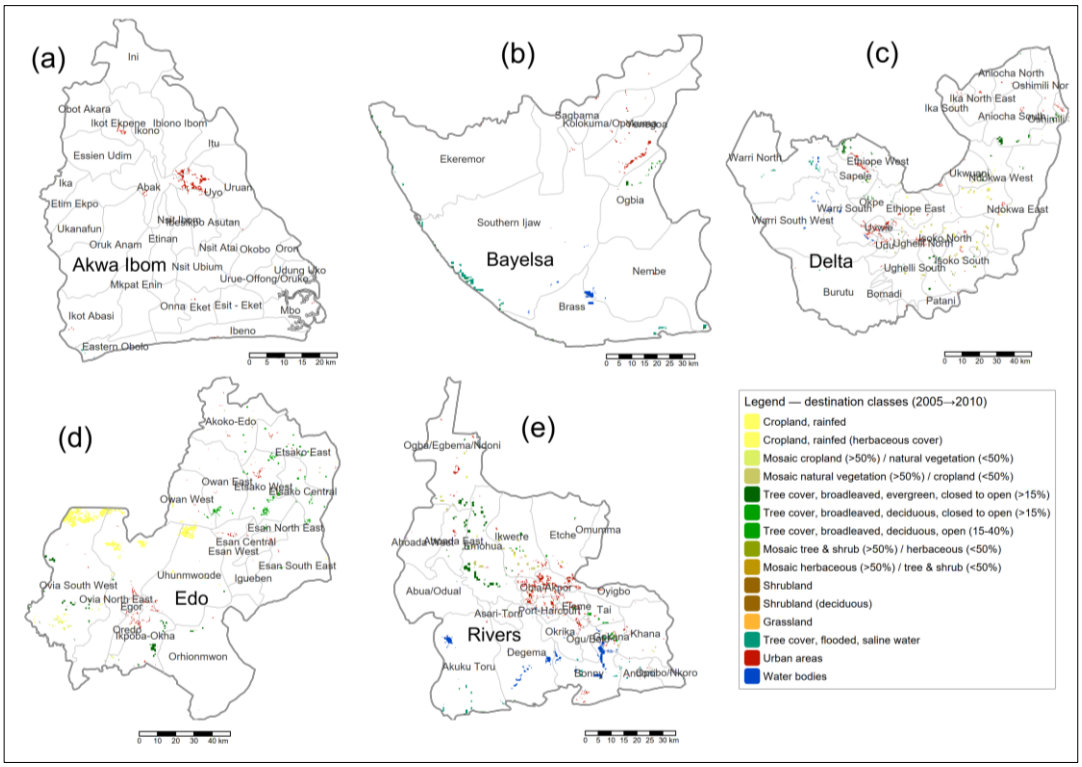

Figure 5. Dominant land use/land cover transitions (2005–2010) in the South–South states of Nigeria: (a) Akwa Ibom, (b) Bayelsa, (c) Delta, (d) Edo, and (e) Rivers, highlighting major flows including cropland expansion, urban growth, and localized forest and wetland conversions.

Akwa Ibom (total change: 21.82 km²). The signal is overwhelmingly urban expansion sourced from agricultural and mosaic classes: 10→190 (12.29 km²; 56.3%), 40→190 (2.76 km²; 12.7%), 30→190 (2.32 km²; 10.6%), with smaller contributions from 62→190 (1.16 km²; 5.3%) and 120→190 (0.89 km²; 4.1%). Hydro-transitions were minor (e.g., 170→190 0.53 km²; 2.45%). Overall, ~93% of change routes into Urban, consistent with rapid peri-urbanization.

Bayelsa (total change: 61.75 km²). Change is dominated by hydro-mangrove dynamics, not urbanization. The largest flows are 210→170 (Water → Tree cover, flooded, saline; 24.96 km²; 40.4%) and 210→50 (Water → Evergreen broadleaved trees; 7.49 km²; 12.1%), alongside 170→210 (11.41 km²; 18.5%). Urban gains occur from multiple sources but remain secondary (e.g., 50→190 5.17 km²; 8.37%; 10→190 3.56 km²; 5.77%; 40→190 2.76 km²; 4.47%).

Delta (total change: 217.70 km²). A diversified vegetation–agriculture turnover dominates, with important two-way exchanges among mosaics and forests and steady urban growth. Major flows include 50→40 (Evergreen trees → Mosaic nat. veg.; 23.14 km²; 10.6%), 40→50 (Mosaic nat. veg. → Evergreen trees; 19.13 km²; 8.79%), 10→190 (Cropland → Urban; 17.61 km²; 8.09%), 170→210 (Saline flooded trees → Water; 14.68 km²; 6.74%), 30→50 (15.21 km²; 6.99%), and 60→40 (12.28 km²; 5.64%). Urbanization is multi-sourced (e.g., 170→190 8.99 km²; 4.13%; 100→190 5.69 km²; 2.62%; 130→190 5.51 km²; 2.53%), but the state's signature remains forest–mosaic restructuring with notable hydrological shifts.

Edo (total change: 432.09 km²). The pattern is dominated by structural vegetation reconfiguration, especially from evergreen forest into herbaceous cropland signals: the singularly largest flow is 50→11 (Evergreen trees → Cropland, herbaceous cover; 189.21 km²; 43.8%), followed by 50→10 (35.96 km²; 8.32%) and 120→62 (Shrubland → Deciduous open; 35.32 km²; 8.17%). Additional exchanges—40→50 (23.37 km²; 5.41%), 50→30 (24.25 km²; 5.61%)—point to canopy thinning and mosaic consolidation. Urban gains are present but modest relative to vegetation shifts (e.g., 10→190 24.07 km²; 5.57%; 62→190 7.29 km²; 1.69%).

Rivers (total change: 245.71 km²). Change reflects a mixed hydrological–forest dynamic: the largest transition is 170→210 (Saline flooded trees → Water; 54.54 km²; 22.2%), alongside strong mosaic-to-forest consolidation (40→50; 32.51 km²; 13.23%) and steady urban accretion from multiple sources (40→190 21.91 km²; 8.92%; 10→190 11.85 km²; 4.82%; 62→190 11.22 km²; 4.57%; 170→190 13.10 km²; 5.33%). Reciprocal water–mangrove shifts (210→170 15.69 km²; 6.38%) underline coastal dynamism.

3.2.3 Dominant flows (2010–2015)

Urban expansion accelerated in Akwa Ibom and remained broad-based in Delta and Rivers, drawing from cropland, mosaics, shrubs, and flooded classes. Hydrological turnover (water ↔ flooded saline trees) is the dominant control in Bayelsa and Rivers, and remains non-trivial in Delta, consistent with deltaic processes and interannual water-extent variability. Vegetation restructuring—particularly evergreen → herbaceous cropland and shrub ↔ deciduous open—is again most pronounced in Edo, pointing to shifts in canopy density/composition at 300 m resolution rather than wholesale clearing alone (Figure 6).

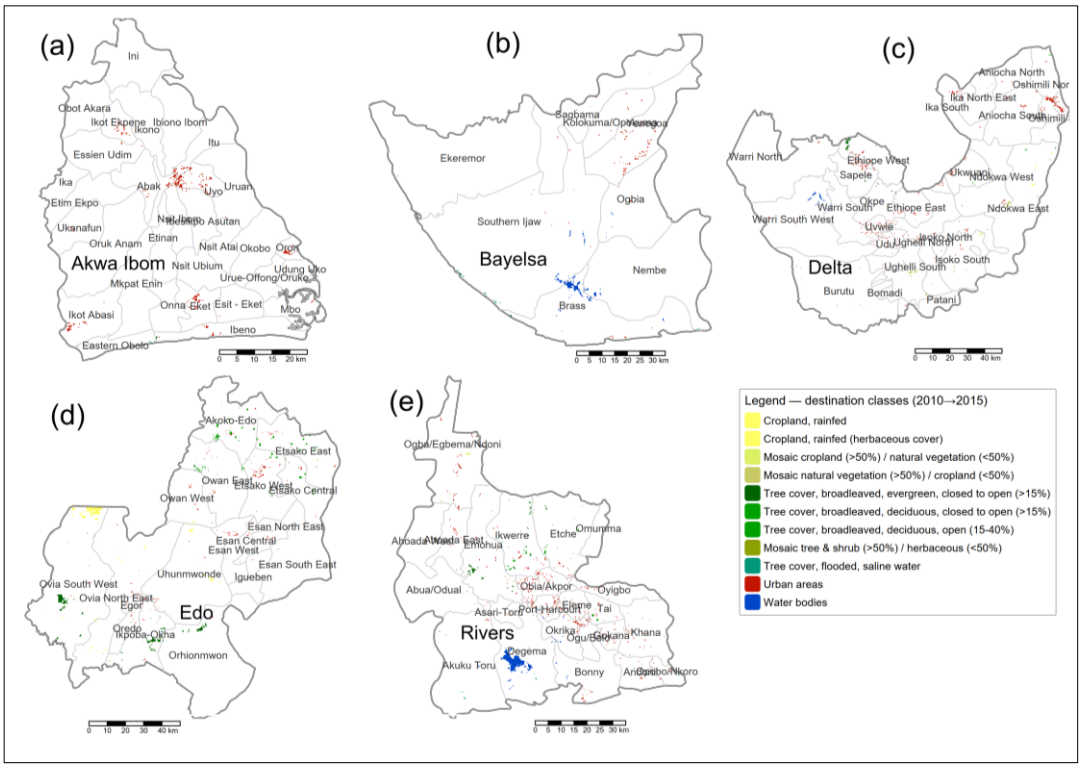

Figure 6. Dominant land use/land cover transitions (2010–2015) across the South–South states of Nigeria: (a) Akwa Ibom, (b) Bayelsa, (c) Delta, (d) Edo, and (e) Rivers, illustrating major conversion flows including urban expansion, cropland development, and localized forest and wetland changes.

Akwa Ibom (total mapped change: 33.14 km²). Change is dominated by urban expansion from agricultural/mosaic sources: 10→190 (19.95 km²; 60.2%), 30→190 (3.47 km²; 10.5%), 40→190 (2.67 km²; 8.1%), 62→190 (2.05 km²; 6.2%), plus 170→190 (2.76 km²; 8.3%). Non-urban flows are small and dispersed. Net signal: concentrated peri-urban growth.

Bayelsa (41.44 km²). The interval is again hydrologically led: 170→210 (saline flooded trees → water; 22.46 km²; 54.2%) and 210→170 (3.12 km²; 7.5%), with additional 50→210 (2.14 km²; 5.2%). Urban gains occur from several classes—50→190 (4.19 km²; 10.1%), 10→190 (2.85 km²; 6.9%), 40→190 (1.51 km²; 3.7%), 62→190 (1.07 km²; 2.6%)—but remain secondary to the water–mangrove dynamics.

Delta (129.16 km²). A mixed regime of urbanization and vegetation/hydro reconfiguration: the largest single flow is 40→190 (mosaic nat. vegetation → urban; 22.24 km²; 17.2%), followed by 10→190 (18.85 km²; 14.6%). Additional urban gains include 30→190 (6.05 km²; 4.7%), 62→190 (6.05 km²; 4.7%), 120→190 (9.78 km²; 7.6%), 100→190 (4.36 km²; 3.4%), 110→190 (3.20 km²; 2.5%), 50→190 (4.72 km²; 3.7%), and smaller inputs (e.g., 170→190 1.69 km²; 1.3%; 210→190 2.40 km²; 1.9%). Hydrological turnover persists (170→210 11.30 km²; 8.75%). Overall, urban growth is broad-based, fed by cropland, mosaics, shrubs, and flooded classes.

Edo (218.61 km²). The signature remains structural vegetation reconfiguration with targeted urban gains. The dominant transition is 50→11 (evergreen trees → cropland, herbaceous cover; 62.95 km²; 28.8%), complemented by 11→50 (27.55 km²; 12.6%), 30→50 (12.80 km²; 5.85%), and 40→50 (8.27 km²; 3.78%). Shrub dynamics are sizeable, notably 120→62 (26.97 km²; 12.3%). Urbanization is meaningful but subordinate to vegetation restructuring: 10→190 (21.31 km²; 9.75%), 62→190 (7.55 km²; 3.45%), with smaller additions from other sources. Interpretation: canopy thinning / conversion to herbaceous cropland and shrub–deciduous adjustments dominate.

Rivers (142.20 km²). Change is again hydro-forest shaped with steady urban accretion. The largest flow is 170→210 (54.36 km²; 38.2%), followed by 40→190 (21.91 km²; 15.4%). Urban draws also include 10→190 (9.44 km²; 6.64%), 50→190 (3.65 km²; 2.57%), 62→190 (3.92 km²; 2.76%), 100→190 (2.76 km²; 1.94%), and 210→190 (3.30 km²; 2.32%). Vegetation consolidation

persists (e.g., 40→50 8.02 km²; 5.64%; 40→60 5.52 km²; 3.88%). Net: coastal/estuarine dynamism plus multi-source urban growth.

3.2.4 Dominant flows (2015–2022)

A structural rebalancing of woody cover is evident across the delta: mosaic natural vegetation (40) converting to evergreen trees (50) is pervasive (especially Delta and Rivers), while Bayelsa shows the opposite tendency (evergreen → mosaics), consistent with fragmentation or canopy thinning. Urban expansion remains a major, but state-specific component: it is very strong in Akwa Ibom (≈38% of all change) and substantial in Edo (≈20%), while Delta and Rivers show broad-based, moderate urban gains fed by cropland, mosaics, shrubs, and flooded classes. Hydrological turnover continues to shape the coastline and lower delta—particularly Rivers (e.g., 170→210)—but is comparatively modest in Bayelsa during this interval (Figure 7).

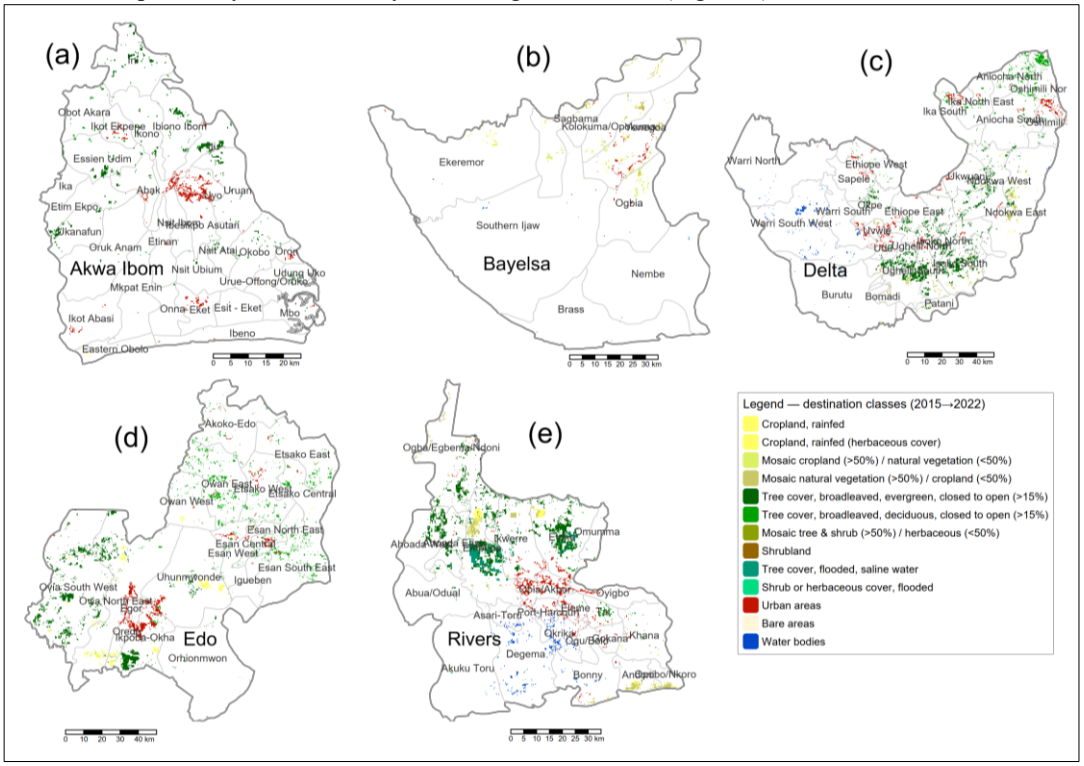

Figure 7. Dominant land use/land cover transitions (2015–2022) in the South–South states of Nigeria: (a) Akwa Ibom, (b) Bayelsa, (c) Delta, (d) Edo, and (e) Rivers, showing major flows such as cropland expansion, urban encroachment, and widespread conversions of forest and vegetation mosaics.

Akwa Ibom (total mapped change: 160.13 km²). Two processes dominate: (i) large movements into evergreen broadleaved tree cover (50) from cropland and mosaics—10→50: 51.47 km² (32.15%), 30→50: 14.25 km² (8.90%), 40→50: 19.95 km² (12.46%)—and (ii) urban expansion from multiple sources—10→190: 45.25 km² (28.26%), 30→190: 5.97 km² (3.73%), 40→190: 4.54 km² (2.84%), with smaller inputs from 50/62/120/122/170→190 (~38% of all change). Interpretation: simultaneous peri-urban growth and consolidation of woody cover at 300 m resolution.

Bayelsa (90.40 km²). Change is concentrated in transitions away from evergreen tree cover (50) toward mosaics—50→30: 31.26 km² (34.58%) and 50→40: 22.97 km² (25.41%)—with additional 50→11 (10.33 km²; 11.43%). Urban gains are present but secondary (e.g., 10→190: 4.45 km²; 4.93%, 50→190: 4.99 km²; 5.52%, 62→190: 5.79 km²; 6.40%; combined ≈19%). Hydrological turnover is modest (170→210: 1.34 km²; 1.48%). Net signal: fragmentation/de-densification of evergreen cover with moderate urban growth.

Delta (883.35 km²). The interval is dominated by vegetation reconfiguration, notably 40→50 (mosaic natural vegetation → evergreen trees; 312.57 km²; 35.38%) and 30→50 (77.59 km²; 8.78%), along with 50→40 (55.89 km²; 6.33%) and 30→60 (46.74 km²; 5.29%). Urbanization is broad-based but secondary (e.g., 10→190: 45.63 km²; 5.17%, 40→190: 49.65 km²; 5.62%,

30→190: 12.18 km²; 1.38%, plus contributions from 50/60/62/100/110/120/170/210→190; combined ≈16–18%). Hydrological exchange persists (170→210: 41.82 km²; 4.73%). Overall: a strong swing toward evergreen cover with significant, spatially distributed urban growth.

Edo (996.36 km²). Very large fluxes originate from cropland (10) toward woody classes—10→50: 260.17 km² (26.11%), 10→60: 190.32 km² (19.10%)—and from evergreen trees (50) toward herbaceous cropland (50→11: 108.14 km²; 10.85%), plus 30→50 (57.40 km²; 5.76%) and 30→60 (34.00 km²; 3.41%). Urbanization is substantial—10→190: 145.72 km² (14.63%) with smaller additions from 30/40/50/60/62/100/110/120/122/130/210→190 (total ≈20% of change). Interpretation: land-system restructuring (cropland–forest–shrub equilibria) with a large, concurrent urban signal.

Rivers (769.45 km²). Changes are led by mosaic↔evergreen and hydro-forest dynamics: 40→50: 328.24 km² (42.66%), 40→170: 80.96 km² (10.52%), 40→190: 72.78 km² (9.46%), 50→40: 57.36 km² (7.45%), 50→11: 34.73 km² (4.51%), and 170→210: 51.42 km² (6.68%). Urban growth draws from many sources—10→190: 18.08 km² (2.35%), 40→190: 72.78 km² (9.46%), 50→190: 5.43 km² (0.71%), 62→190: 5.79 km² (0.75%), 120→190: 8.46 km² (1.10%), 170→190: 9.98 km² (1.30%), etc.—summing to ~16–17%. Net: strong estuarine/forest dynamics with steady multi-source urbanization.

3.3. Land Cover Gains and Losses (2000–2022)

Analysis of land use/land cover (LULC) dynamics across the South–South states of Nigeria revealed marked heterogeneity in gains, losses, and net changes between 2000 and 2022. In **Akwa Ibom**, substantial losses occurred in rainfed cropland (−135.47 km²) and mosaic vegetation–cropland classes (−29.75 km² to −34.55 km²), while notable gains were recorded in **urban areas (+126.48 km²)** and broadleaved evergreen forest (+84.60 km²). This underscores rapid urban expansion around Uyo and adjoining settlements, alongside localized forest regrowth.

In **Bayelsa**, the landscape remained dominated by swamp forests and wetlands, but the balance between forest loss and agricultural expansion was evident. Rainfed cropland declined (−11.67 km²), while mosaic cropland (>50%) gained substantially (+28.68 km²). Evergreen broadleaved forest experienced major decline (−62.25 km²), offset partly by increases in saline water tree cover (+2.85 km²). Urban growth (+46.05 km²) was concentrated around Yenagoa and other local government areas, whereas water bodies declined markedly (−18.45 km²).

Delta State exhibited the most extensive changes, with major declines in mosaic natural vegetation (−352.66 km²), saline water tree cover (−72.17 km²), and shrubland (−36.09 km²). Conversely, evergreen broadleaved forest expanded considerably (+364.13 km²), and urban areas recorded the highest gain among all states (+361.41 km²), reflecting rapid population growth and industrial expansion around Warri, Ughelli, and Asaba.

In **Edo**, rainfed cropland experienced the largest net loss (−403.94 km²), while rainfed cropland with herbaceous cover expanded substantially (+495.62 km²). Evergreen broadleaved forest declined sharply (−501.78 km²), but deciduous forest classes showed strong recovery, with closed-to-open (+386.08 km²) and open forests (+586.92 km²) indicating vegetation succession and forest transition processes. Urban growth (+393.78 km²) was also significant, largely in Benin City and surrounding peri-urban zones.

Rivers State showed major reductions in mosaic natural vegetation (−517.69 km²) and saline water tree cover (−103.69 km²), alongside losses in shrubland (−29.93 km²). However, gains were substantial in evergreen broadleaved forest (+326.63 km²) and water bodies (+128.24 km²). Urban expansion was pronounced (+314.56 km²), reflecting the growth of Port Harcourt and adjoining industrial settlements.

Collectively, the results highlight a strong **urbanization trajectory across all states**, with urban gains exceeding 1,240 km², accompanied by widespread **loss of mosaic vegetation and shrublands**. While some areas exhibited forest regrowth, particularly evergreen and deciduous

classes, these were often localized and spatially fragmented. The findings underscore the trade-offs between agricultural expansion, urban growth, and ecosystem integrity in one of Nigeria's most socioeconomically dynamic regions.

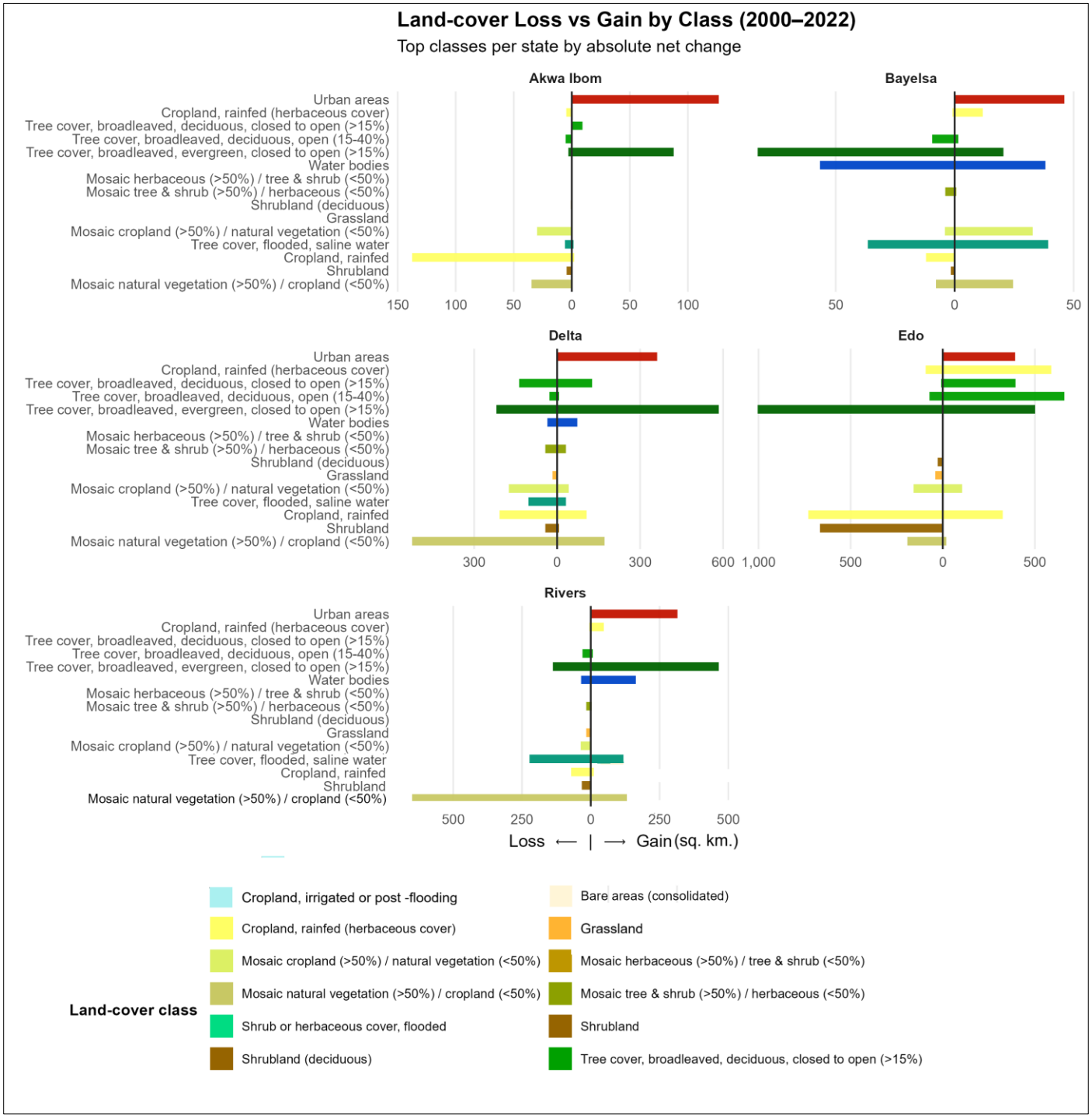

Figure 8. Landcover loss vs Gain by Class

4. Discussion

Our results demonstrate that land-cover change in the South–South zone of Nigeria is both spatially heterogeneous and functionally significant, reflecting the combined pressures of urbanization, agricultural expansion, coastal hydrodynamics, and forest restructuring (Adelekan et al., 2020; Seto & Fragkias, 2011). The most striking outcome is the rapid growth of urban areas across all states, with cumulative expansion exceeding 1,240 km² over two decades. This trajectory aligns with Nigeria's status as one of Africa's fastest-urbanizing countries, where population growth and infrastructure development are transforming peri-urban landscapes into continuous built-up corridors (World Bank, 2023; Abiodun et al., 2021). The marked increases in Edo and Rivers, in particular, underscore the role of state capitals (Benin City and Port Harcourt) as regional economic magnets, while smaller but notable gains in Akwa Ibom and Bayelsa highlight peri-urban expansion into previously rural settings. These findings echo recent studies linking urbanization in the Niger Delta to both oil-sector investments and rural-to-urban migration (Onyena & Sam, 2020).

Beyond urban growth, forest dynamics reveal nuanced, state-specific trajectories. Delta and Rivers recorded substantial increases in evergreen broad-leaved forests, possibly reflecting secondary succession, reforestation initiatives, or classification refinements where mosaics consolidate into homogeneous forest patches (Ayanlade et al., 2018). Conversely, Edo experienced a pronounced decline in evergreen forest (−502 km²) but simultaneous expansion of open deciduous forest (+587 km²), suggesting structural transformation rather than wholesale loss, consistent with selective logging and canopy thinning observed across southern Nigeria (Okeke & Adegoke, 2021). The stability of flooded saline forests in Bayelsa and Rivers, despite localized turnover, reinforces mangrove ecosystem resilience, although modest net declines (e.g., Rivers: −104 km²) point to vulnerability from coastal reclamation, aquaculture, and oil-related disturbance (Bunting et al., 2018; Nwilo et al., 2022).

The contraction of mosaic classes across all states is particularly significant. These heterogeneous landscapes—intermixing cropland, shrubland, and natural vegetation—function as transitional buffers supporting ecosystem services and livelihoods (Turner et al., 2020). Their decline indicates land-system simplification, consistent with broader regional evidence that mosaics in West Africa are increasingly replaced by uniform cropland or urban land under demographic and market pressures (van Vliet et al., 2020; Brandt et al., 2021). In the South–South zone, the implications are twofold: consolidation into forest enhances carbon sequestration, whereas conversion to cropland or urban land reduces biodiversity and soil stability.

Hydrological and coastal processes remain central to explaining land-cover dynamics in Bayelsa, Delta, and Rivers. Reciprocal transitions between water bodies and flooded saline tree cover indicate mangrove shoreline adjustments driven by fluctuating hydroperiods and tidal regimes (Bunting et al., 2018; Woodroffe et al., 2016). These patterns mirror estuarine morphodynamics documented for the Niger Delta, where sedimentation, erosion, and seasonal flooding reshape wetland–water interfaces. The relative stability of open-water fractions, with localized expansions in Rivers and Delta, may also reflect riverine flooding and subsidence, processes projected to intensify with sea-level rise and climate variability (IPCC, 2023).

Collectively, these findings highlight a trade-off between urbanization and ecosystem integrity. While Delta and Rivers show localized forest gains, these are often fragmented and offset by mosaic and shrubland losses. Urban expansion—though still below 5 % of total area—is accelerating, with implications for heat exposure, runoff, and land degradation. Policy priorities should therefore focus on (i) protecting mangrove and swamp forests as natural flood buffers, (ii) regulating peri-

urban sprawl, and (iii) restoring degraded mosaics to sustain ecological diversity (Feka & Ajonina, 2011).

By employing interval-resolved flow analysis, this study captures not only what has changed but how transitions occur, offering the first state-level, multi-decadal LULC assessment of the South–South zone using C3S/CCI data. The baseline supports climate adaptation, urban governance, and ecosystem restoration strategies in one of Nigeria's most environmentally dynamic regions (Elvidge et al., 2020).

5. Conclusions

This study provides the first state-wise, multi-decadal assessment of land-cover change in Nigeria's South–South zone using C3S/CCI data (2000–2022). The results reveal a clear trajectory of accelerating urban expansion, localized but significant forest restructuring, widespread loss of mosaics and shrublands, and persistent hydro-mangrove turnover along the delta. While some areas show gains in evergreen and deciduous forests, these are often fragmented and offset by landscape simplification. The findings underscore the trade-offs between rapid development and ecosystem stability, highlighting the need for integrated land-use planning, mangrove conservation, and targeted restoration interventions to sustain ecological resilience in one of West Africa's most dynamic regions.

Supplementary Materials: Available at https://github.com/zubairgis/nigeria-hensard

Data Availability Statement: The satellite data used in this study are open to access as follows:

Administrative: https://developers.google.com/earth-engine/datasets/catalog/ FAO/GAUL/2015/level1
DEM:https://developers.google.com/earth-engine/datasets/catalog/ SGS/SRTMGL1_003
Roads & Water Routes: https://www.openstreetmap.org/#map=6/9.12/8.67
Landcover classes: https://land.copernicus.eu/en/global
Google Building Footprints: https://sites.research.google/gr/open-buildings/

Author Contributions: Conceptualization, Z.I. and Y.J.C.; methodology, Z.I. F.M. and U.U.E.; formal analysis, Z.I., Y.J.C., and R.K.H.; investigation, U.U.E., Y.J.D., F.M. and R.K.H.; data curation, U.U.E. and E.L.E.; writing original draft preparation, Z.I. and Y.J.C.; writing—review and editing, U.U.E., E.L.E., and R.K.H.; supervision, Z.I.; project administration, Z.I. F.M.and Y.J.C. All authors have read and agreed to the published version of the manuscript.

Funding

This research received no external funding.

Informed Consent Statement

Not applicable.

Conflicts of Interest

The authors declare no conflict of interest.

Abbreviations

The following abbreviations are used in this manuscript:

GEE	Google Earth Engine
GIS	Geographic Information System
LULC	Land Use/Land Cover
WHO	World Health Organisation
DEM	Digital Elevation Model

References

Abiodun, B. J., Adeola, A. M., & Ogunjobi, K. O. (2021). Urban expansion and heat stress over Nigerian cities: Implications for sustainable development. Sustainable Cities and Society, 74, 103257. https://doi.org/10.1016/j.scs.2021.103257

Adejuwon, J. O. (2012). Rainfall seasonality in the Niger Delta Belt, Nigeria. Journal of Geography and Regional Planning, 5(2), 51–60. https://doi.org/10.5897/JGRP11.114

Adelekan, I. O., Johnson, C., Manda, M. A. Z., & Parnell, S. (2020). The urban climate challenge in Africa. Current Opinion in Environmental Sustainability, 46, 1–9. https://doi.org/10.1016/j.cosust.2020.07.001

Aigbe, H. I., & Ewemade, F. O. (2019). Deforestation and degradation of mangrove forests in the Niger Delta region of Nigeria. Environmental Monitoring and Assessment, 191(11), 664. https://doi.org/10.1007/s10661-019-7774-5

Aigbe, H. I., & Ogundele, F. O. (2020). Urban expansion and the challenges of sustainable development in the Niger Delta. Urban Science, 4(3), 31. https://doi.org/10.3390/urbansci4030031

Akani, G. C., Luiselli, L., & Angelici, F. M. (2015). Biodiversity and conservation of the Niger Delta region of Nigeria: An overview. Applied Ecology and Environmental Research, 13(4), 909–928. https://doi.org/10.15666/aeer/1304_909928

Arino, O., Bicheron, P., Achard, F., Latham, J., Witt, R., & Weber, J.-L. (2012). GlobCover 2009: ESA Living Planet Symposium Report. European Space Agency.

Ayanlade, A., & Proske, U. (2016). Assessing wetland degradation and loss of ecosystem services in the Niger Delta, Nigeria. Environmental Monitoring and Assessment, 188(3), 161. https://doi.org/10.1007/s10661-016-5119-5

Ayanlade, A., Radeny, M., & Morton, J. F. (2018). Agricultural land use and vegetation dynamics in southern Nigeria. Land Degradation & Development, 29(10), 3472–3484. https://doi.org/10.1002/ldr.3139

Bontemps, S., Defourny, P., Bogaert, E. V., Arino, O., Kalogirou, V., & Perez, J. R. (2011). GLOBCOVER 2009—Products description and validation report. European Space Agency.

Borner, J., Schulz, C., & von Luxburg, U. (2020). Land use dynamics and urban expansion in coastal West Africa: Mapping 30 years of change using Landsat imagery. Remote Sensing, 12(11), 1780. https://doi.org/10.3390/rs12111780

Brandt, M., Tong, X., Tian, F., Liu, Y. Y., & Fensholt, R. (2021). The human-environment nexus in the Sahel: Land-cover transitions and drivers. Nature Sustainability, 4(8), 664–672. https://doi.org/10.1038/s41893-021-00709-x

Buchhorn, M., Smets, B., Bertels, L., De Roo, B., Lesiv, M., Tsendbazar, N. E., Herold, M., & Fritz, S. (2020). Copernicus Global Land Service: Land Cover 100 m: Collection 3: Epoch 2019: Globe. Zenodo. https://doi.org/10.5281/zenodo.3939050

Bunting, P., Rosenqvist, A., Lucas, R. M., Rebelo, L. M., Hilarides, L., Thomas, N., ... & Finlayson, C. M. (2018). Global mangrove extent change 1996–2010: The Mangrove Forests of the World dataset. Global Ecology and Biogeography, 27(8), 971–986. https://doi.org/10.1111/geb.12795

Chen, J., Ban, Y., & Li, S. (2020). Open access to Earth observation data for global land-cover mapping and monitoring. International Journal of Digital Earth, 13(2), 177–200. https://doi.org/10.1080/17538947.2019.1598803

Chukwu, G. O., Akpan, P. E., & Ochege, F. U. (2023). Land use/land cover change and its implications on carbon sequestration in the Niger Delta region of Nigeria. Carbon Management, 14(1), 225–240. https://doi.org/10.1080/17583004.2023.2184142

Congalton, R. G., & Green, K. (2019). Assessing the Accuracy of Remotely Sensed Data: Principles and Practices (3rd ed.). CRC Press. https://doi.org/10.1201/9780429052729

Defourny, P., Lamarche, C., & Bontemps, S. (2017). ESA Climate Change Initiative Land Cover (CCI LC): Product User Guide, Version 2. European Space Agency. https://maps.elie.ucl.ac.be/CCI/viewer/download/ESACCI-LC-Ph2-PUGv2_2.0.pdf

Elvidge, C. D., Zhizhin, M., Ghosh, T., & Hsu, F. C. (2020). Annual patterns of nighttime light and their implications for urban growth monitoring in Africa. Remote Sensing, 12(6), 951. https://doi.org/10.3390/rs12060951

Emoyan, O. O., Akpoborie, I. A., & Akporhonor, E. E. (2008). Environmental pollution in the Niger Delta, Nigeria. Interdisciplinary Journal of Environmental Research, 2(3), 53–60.

Etuonovbe, A. K. (2011). The devastating effects of flooding in Nigeria. FIG Working Week 2011—Bridging the Gap Between Cultures, Marrakech, Morocco, 18–22 May 2011.

Eze, E. B., Ezemonye, M. N., & Ogedengbe, K. (2021). Urbanization and flood risk in the Niger Delta coastal region of Nigeria. Natural Hazards, 108(2), 2059–2080. https://doi.org/10.1007/s11069-021-04722-0

FAO. (2015). Global Administrative Unit Layers (GAUL): Technical Aspects of the GAUL Dataset. Food and Agriculture Organization of the United Nations. https://data.apps.fao.org/map/catalog/srv/en/main.home

Feka, N. Z., & Ajonina, G. N. (2011). Drivers causing decline of mangrove in West-Central Africa: A review. International Journal of Biodiversity Science, Ecosystem Services & Management, 7(3), 217–230. https://doi.org/10.1080/21513732.2011.634436

Griffiths, P., van der Linden, S., Kuemmerle, T., & Hostert, P. (2019). A pixel-based Landsat compositing algorithm for large area land-cover mapping. IEEE Journal of Selected Topics in Applied Earth Observations and Remote Sensing, 12(1), 388–397. https://doi.org/10.1109/JSTARS.2018.2879750

Hansen, M. C., Krylov, A., Tyukavina, A., Potapov, P. V., Turubanova, S. A., Zutta, B. R., & Moore, R. (2016). Humid tropical forest disturbance alerts using Landsat data. Environmental Research Letters, 11(3), 034008. https://doi.org/10.1088/1748-9326/11/3/034008

Herold, M., Mayaux, P., Woodcock, C. E., Baccini, A., & Schmullius, C. (2008). Some challenges in global land-cover mapping: An assessment of agreement and accuracy in existing 1 km datasets. Remote Sensing of Environment, 112(5), 2538–2556. https://doi.org/10.1016/j.rse.2007.11.013

Hijmans, R. J. (2023). terra: Spatial data analysis. R package version 1.7-78. https://CRAN.R-project.org/package=terra

Hollmann, R., Merchant, C. J., Saunders, R., Downy, C., Buchwitz, M., Cazenave, A., ... & Defourny, P. (2013). The ESA Climate Change Initiative: Satellite data records for essential climate variables. Bulletin of the American Meteorological Society, 94(10), 1541–1552. https://doi.org/10.1175/BAMS-D-11-00254.1

IPCC. (2023). Climate Change 2023: Synthesis Report. Contribution of Working Groups I, II and III to the Sixth Assessment Report of the Intergovernmental Panel on Climate Change. IPCC Secretariat. https://www.ipcc.ch/report/ar6/syr

Kuenzer, C., Bluemel, A., Gebhardt, S., Quoc, T. V., & Dech, S. (2011). Remote sensing of mangrove ecosystems: A review. Remote Sensing, 3(5), 878–928. https://doi.org/10.3390/rs3050878

Li, W., Ciais, P., MacBean, N., Defourny, P., & Hartley, A. (2020). Mapping global land-cover transitions from 1992 to 2018 using ESA CCI data. Earth System Science Data, 12(3), 295–310. https://doi.org/10.5194/essd-12-295-2020

Lu, D., Mausel, P., Brondizio, E., & Moran, E. (2014). Change detection techniques. International Journal of Remote Sensing, 25(12), 2365–2401. https://doi.org/10.1080/0143116031000139863

Mmom, P. C., & Fred-Ahmadu, O. H. (2020). Geospatial assessment of land use dynamics and ecosystem degradation in the Niger Delta, Nigeria. Environmental Challenges, 1, 100005. https://doi.org/10.1016/j.envc.2020.100005

Moser, G., Serpico, S. B., & Benediktsson, J. A. (2020). Land-cover change detection via unsupervised deep feature learning. IEEE Transactions on Geoscience and Remote Sensing, 58(10), 7374–7387. https://doi.org/10.1109/TGRS.2020.2981236

Numbere, A. O., & Camilo, G. R. (2018). Mangrove leaf litter decomposition under changing tidal flooding regimes in the Niger Delta, Nigeria. Wetlands Ecology and Management, 26(4), 491–503. https://doi.org/10.1007/s11273-018-9591-1

Nwankwoala, H. O. (2015). Causes of hydrological hazards in the Niger Delta region of Nigeria. International Journal of Environment and Pollution Research, 3(3), 1–17.

Nwilo, P. C., & Olayinka, D. N. (2020). Assessment of river network changes and hydrological implications in coastal Nigeria using remote sensing. Hydrological Sciences Journal, 65(11), 1871–1883. https://doi.org/10.1080/02626667.2020.1785832

Nwilo, P. C., Badejo, O. T., & Olayinka, D. N. (2021). Mapping shoreline changes and coastal erosion in Nigeria's Niger Delta using multi-temporal satellite imagery. Marine Geodesy, 44(2), 133–151. https://doi.org/10.1080/01490419.2021.1881407

Nwilo, P. C., Olayinka, D. N., & Adzandeh, A. E. (2019). Shoreline change and its environmental implications in the Niger Delta region of Nigeria. Ocean & Coastal Management, 181, 104896. https://doi.org/10.1016/j.ocecoaman.2019.104896

Odekunle, T. O. (2010). An assessment of the influence of the inter-tropical discontinuity on rainfall distribution in Nigeria. Theoretical and Applied Climatology, 100(3–4), 431–442. https://doi.org/10.1007/s00704-009-0184-6

Odjugo, P. A. O. (2011). Regional evidence of climate change in Nigeria. Journal of Geography and Regional Planning, 4(6), 142–150. https://doi.org/10.5897/JGRP10.139

Okeke, F. I., & Adegoke, J. O. (2021). Patterns and drivers of forest cover change in southern Nigeria. Environmental Monitoring and Assessment, 193(10), 662. https://doi.org/10.1007/s10661-021-09493-x

Okeke, O. C., Udoh, J. I., & Eze, B. E. (2021). Land cover change detection and forest loss estimation in the Niger Delta using multi-temporal Landsat imagery. Geocarto International, 36(21), 2521–2540. https://doi.org/10.1080/10106049.2020.1726500

Olofsson, P., Foody, G. M., Herold, M., Stehman, S. V., Woodcock, C. E., & Wulder, M. A. (2014). Good practices for estimating area and assessing accuracy of land-change maps. Remote Sensing of Environment, 148, 42–57. https://doi.org/10.1016/j.rse.2014.02.015

Onyena, A. P., & Sam, K. O. (2020). The impact of oil exploitation on urbanization patterns in the Niger Delta region of Nigeria. Environmental Challenges, 1, 100008. https://doi.org/10.1016/j.envc.2020.100008

Poulter, B., MacBean, N., Hartley, A., Khlystova, I., Arino, O., Betts, R., ... & Jones, C. D. (2015). Plant functional type classification for earth system models: CCI Land Cover product and MODIS data. Remote Sensing of Environment, 190, 108–123. https://doi.org/10.1016/j.rse.2016.12.002

Santoro, M., Cartus, O., Carvalhais, N., Rozendaal, D. M. A., Avitabile, V., Araza, A., ... & Herold, M. (2021). The global forest above-ground biomass pool for 2010 estimated from high-resolution satellite observations. Earth System Science Data, 13(9), 3927–3950. https://doi.org/10.5194/essd-13-3927-2021

Seto, K. C., & Fragkias, M. (2011). Quantifying spatiotemporal patterns of urban land-use change in Asia and Africa. Remote Sensing of Environment, 114(8), 1729–1736. https://doi.org/10.1016/j.rse.2010.04.003

Smith, G. M., Foody, G. M., & Atkinson, P. M. (2019). Accuracy and uncertainty in land cover change detection. Progress in Physical Geography, 43(6), 789–817. https://doi.org/10.1177/0309133319883652

Spalding, M. D., Kainuma, M., & Collins, L. (2010). World Atlas of Mangroves (2nd ed.). Earthscan. https://doi.org/10.4324/9781849776608

Turner, B. L., Lambin, E. F., & Reenberg, A. (2020). The emergence of land-system science for global environmental change and sustainability. Proceedings of the National Academy of Sciences, 117(12), 6628–6636. https://doi.org/10.1073/pnas.1922190117

Udo, S. O., & Akinyemi, F. O. (2022). Spatiotemporal dynamics of urban growth and vegetation loss in Port Harcourt metropolis, Nigeria. Environmental Challenges, 7, 100486. https://doi.org/10.1016/j.envc.2022.100486

Uluocha, N. O., & Okeke, I. C. (2004). Implications of wetlands degradation for water resources management: Lessons from Nigeria. GeoJournal, 61(2), 151–154. https://doi.org/10.1007/s10708-004-2868-3

van Vliet, J., Bregt, A. K., Brown, C., van Delden, H., Heckbert, S., & Verburg, P. H. (2020). A review of current and future land-use modeling. Environmental Modelling & Software, 134, 104818. https://doi.org/10.1016/j.envsoft.2020.104818

Wessels, K. J., van den Bergh, F., & Scholes, R. J. (2016). Limits to detectability of land degradation by trend analysis of vegetation index data. Remote Sensing of Environment, 125, 10–22. https://doi.org/10.1016/j.rse.2012.06.022

Woodcock, C. E., Loveland, T. R., Herold, M., & Bauer, M. E. (2020). Transitioning from change detection to monitoring with Landsat data. Remote Sensing of Environment, 238, 111622. https://doi.org/10.1016/j.rse.2019.111622

Woodroffe, C. D., Rogers, K., McKee, K. L., Lovelock, C. E., Mendelssohn, I. A., & Saintilan, N. (2016). Mangrove sedimentation and response to relative sea-level rise. Annual Review of Marine Science, 8, 243–266. https://doi.org/10.1146/annurev-marine-122414-034025

World Bank. (2023). Nigeria Urbanization Review: Pathways to Sustainable Urban Growth. Washington, DC: World Bank Group. https://doi.org/10.1596/978-1-4648-1942-1

Wulder, M. A., Loveland, T. R., Roy, D. P., Crawford, C. J., Masek, J. G., Woodcock, C. E., ... & Zhu, Z. (2018). Current status of Landsat program, science, and applications. Remote Sensing of Environment, 225, 127–147. https://doi.org/10.1016/j.rse.2018.04.015